

A search for diffuse bands in fullerene planetary nebulae: evidence of diffuse circumstellar bands

J. J. Díaz-Luis^{1,2}, D. A. García-Hernández^{1,2}, N. Kameswara Rao^{1,2,3}, A. Manchado^{1,2,4}, and F. Cataldo^{5,6}

¹ Instituto de Astrofísica de Canarias, C/ Via Láctea s/n, E-38205 La Laguna, Spain e-mail: jdiaz@iac.es, agarcia@iac.es

² Departamento de Astrofísica, Universidad de La Laguna (ULL), E-38206 La Laguna, Spain

³ Indian Institute of Astrophysics, Bangalore 560034, India; nkrao@iiap.res.in

⁴ Consejo Superior de Investigaciones Científicas, Madrid, Spain

⁵ INAF- Osservatorio Astrofisico di Catania, Via S. Sofia 78, Catania 95123, Italy

⁶ Actinium Chemical Research srl, Via Casilina 1626/A, 00133 Rome, Italy

Received xx, 2014; accepted xx x, 2014

ABSTRACT

Large fullerenes and fullerene-based molecules have been proposed as carriers of diffuse interstellar bands (DIBs). The recent detection of the most common fullerenes (C_{60} and C_{70}) around some planetary nebulae (PNe) now enable us to study the DIBs towards fullerene-rich space environments. We search DIBs in the optical spectra towards three fullerene-containing PNe (Tc 1, M 1-20, and IC 418). Special attention is given to DIBs which are found to be unusually intense towards these fullerene sources. In particular, an unusually strong 4428 Å absorption feature is a common characteristic of fullerene PNe. Similar to Tc 1, the strongest optical bands of neutral C_{60} are not detected towards IC 418. Our high-quality ($S/N > 300$) spectra for PN Tc 1, together with its large radial velocity, permit us to search for the presence of diffuse bands of circumstellar origin, which we refer to as diffuse circumstellar bands (DCBs). We report the first tentative detection of two DCBs at 4428 and 5780 Å in the fullerene-rich circumstellar environment around the PN Tc 1. Laboratory and theoretical studies of fullerenes in their multifarious manifestations (carbon onions, fullerene clusters, or even complex species formed by fullerenes and other molecules like PAHs or metals) may help solve the mystery of some of the diffuse band carriers.

Key words. Astrochemistry — Line: identification — circumstellar matter — ISM: molecules — planetary Nebulae: individual: Tc 1, M 1-20, IC 418

1. Introduction

Identification of the carriers of the diffuse interstellar bands (DIBs) has been very elusive since they were first discovered by Heger (1922), who first noted their stationary nature as observed towards a spectroscopic binary, indicating that their origin was not stellar but rather interstellar. Since then, more than 380 bands have been identified (e.g., Hobbs et al. 2008), and they have been associated to the interstellar medium (ISM) because their strengths show a positive relationship with the observed extinction (Merrill & Wilson 1936), as well as to the neutral sodium column density (Herbig 1993). Most of the DIBs are located in the 4000 to 10000 Å wavelength range¹. Different complex carbon-based molecules - e.g., carbon chains, polycyclic aromatic hydrocarbons (PAHs), and fullerenes - have been proposed as DIB's carriers (see, e.g., Cox 2011 for a review).

The link between PAHs and DIBs was made by Crawford et al. (1985), Leger & d'Hendecourt (1985), and Van der Zwet & Allamandola (1985). Apart from having (electronic) transitions in the UV, optical, and near infrared, PAHs are also very resistant to UV radiation. Thus, the expected high abundance of PAHs in space, their optical absorption spectrum, and the presence of substructure in the DIB profiles, seem to give support for the PAH-DIB hypothesis (see, e.g., Salama et al. 1999, Cox 2011).

¹ Geballe et al. (2011) report 13 newly discovered DIBs in the near-infrared region at the H-band (1.5-1.8 micrometre interval) on high-extinction sightlines towards stars in the Galactic centre.

However, a potential problem with the PAH-DIB hypothesis is the lack of interstellar bands in the UV part of the astronomical spectra (Snow & McCall 2006; Snow & Destree 2011), where strong PAH transitions are expected (see, e.g., Tielens 2008).

Fullerenes and fullerene-related molecules (Kroto et al. 1985) are presented as an alternative to the PAH-DIB hypothesis. The remarkable stability of fullerenes against intense radiation (e.g., Cataldo et al. 2009) suggests that fullerenes may be present in the ISM. The most common fullerenes (C_{60} and C_{70}) have recently been detected in a variety of space environments, such as planetary nebulae (PNe) (Cami et al. 2010; García-Hernández et al. 2010, 2011a, 2012a), reflection nebulae (Sellgren et al. 2010), a proto-PN (Zhang & Kwok 2011), and the two least H-deficient R Coronae Borealis stars (García-Hernández et al. 2011b,c). The recent detection of fullerenes in PNe with normal H-abundances (García-Hernández et al. 2010) indicates that fullerenes are common around evolved stars and that they should be widespread in the ISM. Indeed, the 9577 and 9632 Å DIBs observed in a few reddened stars lie near two electronic transitions of the C_{60}^+ cation observed in rare gas matrices (Foing & Ehrenfreund 1994). More recently, Iglesias-Groth & Esposito (2013) have reported the detection of the 9577 and 9632 Å DIBs in the fullerene-containing proto-PN IRAS 01005+7910, and they suggest the C_{60}^+ cation as their carrier. However, a confirmation of the proposal that C_{60}^+ could be the carrier of these two DIBs still awaits spectroscopic gas-phase C_{60}^+ laboratory data. The detection of C_{60}^+ through its infrared vibrational bands

in the NGC 7023 reflection nebula with the *Spitzer space telescope* could support the idea of C_{60}^+ being a DIB carrier (Berné et al. 2013, 2014), but these C_{60}^+ infrared bands are not seen in the *Spitzer* spectrum of the proto-PN IRAS 01005+7910 (see, e.g., Zhang & Kwok 2011).

At present, very little is known about the presence of the DIB carriers in other astrophysical environments (e.g., Cox 2011). If the DIBs arise from large gas phase molecules, such as PAHs and fullerenes, then they are also expected to be present in other carbon-rich space environments like circumstellar shells around stars. Diffuse circumstellar bands (DCBs) in absorption have been unsuccessfully studied for more than 40 years (Seab 1995)². DCBs are absent in the dusty circumstellar envelopes (with or without PAH-like features) of AGB/post-AGB stars, as well as in the atmospheres of cool stars and Herbig Ae/Be stars (Seab 1995; Cox 2011; Luna et al. 2008). Thus, the conventional wisdom is that there are no diffuse bands in circumstellar environments. The unambiguous detection of DCBs would have a strong impact on diffuse bands theories; for example, they can be compared to the presence of the proposed diffuse band carriers mentioned above. The main difficulty to detect DCBs is to distinguish them from the DIBs (Seab 1995; Cox 2011). This distinction can only be made by measuring the radial velocities of the circumstellar and interstellar components. Here we search for the possible presence of DCBs in a selected sample of three fullerene-containing PNe.

In García-Hernández & Díaz-Luis (2013), we presented some of the new results for DIBs towards the fullerene PNe Tc 1 and M 1-20, and the very broad 4428 Å DIB was found to be unusually intense (based on the measured equivalent widths) towards both Tc 1 and M 1-20. The speculation was offered that the unusually strong 4428 Å DIB towards fullerene PNe may be related to the presence of larger fullerenes and buckyonions in their circumstellar envelopes. However, García-Hernández & Díaz-Luis (2013) did not carry out any radial velocity analysis, something that is mandatory for confirming a circumstellar origin.

In this paper, we present a detailed DIB radial velocity analysis and a complete search of diffuse bands towards three PNe (Tc 1, M 1-20, and IC 418) containing fullerenes and accompanied (or not) by PAH molecules. A summary of the optical spectroscopic observations is presented in Section 2. Section 3 gives a complete analysis of the DIBs towards fullerene PNe, including the normal DIBs most commonly found in the ISM and a few unusually strong DIBs. Section 4 presents our search for DCBs in fullerene PNe and their detection in PN Tc 1. Sections 5 and 6 discuss the non-detection of the electronic C_{60} transitions in the IC 418 optical spectrum and the possible connection between fullerenes and diffuse bands, respectively. The conclusions of our work are given in Section 7.

2. Optical spectroscopy of PNe with fullerenes

We acquired optical spectra of the fullerene PNe Tc 1 ($B=11.1$, $E(B-V)=0.23$; Williams et al. 2008), M 1-20 ($B=13.7$, $E(B-V)=0.80$; Wang & Liu 2007), and IC 418 ($B=9.8$, $E(B-V)=0.23$; Pottasch et al. 2004). The detection of fullerene-like features in the IC 418 *Spitzer* spectrum has recently been reported by Morisset et al. (2012). Tc 1 displays a fullerene-dominated spectrum with no clear signs of PAHs, while M 1-20 and IC 418 also show

² We note that some diffuse bands in emission have been previously seen in a proto-PN (the Red Rectangle) and in the R Coronae Borealis star V854 Cen (see, e.g., Scarrott et al. 1992; Rao & Lambert 1993).

weak PAH-like features (see, e.g., García-Hernández et al. 2010; Meixner et al. 1996). All PNe in our sample also show unidentified broad dust emission features centred at ~ 9 – 13 and 25 – 35 μm (see, e.g., García-Hernández et al. 2012a). The effective temperature of PN IC 418 ($T_{\text{eff}}=36700$ K) is very similar to the one in Tc 1 ($T_{\text{eff}}=34060$ K), while M 1-20 ($T_{\text{eff}}=45880$ K) is among the fullerene PNe with the hottest central stars (Otsuka et al. 2014). Our sample PNe display round or else elliptical morphologies: round (Tc 1) and elliptical (IC 418, M 1-20) (see Figure 1 in Otsuka et al. 2014).

The observations of Tc 1 and M 1-20 were carried out at the ESO VLT (Paranal, Chile) with UVES in service mode between May and September 2011 (see García-Hernández & Díaz-Luis 2013 for more observational details). We used the 2.4" slit centred at the central stars of the two PNe (see Figure 1 in Otsuka et al. 2014) and following the parallactic angle. This configuration should give a resolving power of ~ 15000 from ~ 3300 to 9400 Å. However, from the O_2 telluric lines at ~ 6970 Å, we measure a much higher resolving power of about 37000. The signal-to-noise ratio (S/N) (in the final combined spectrum) in Tc 1 is very high (~ 300 at 4000 Å and >300 at longer wavelengths), which permitted us to search for the expected electronic transitions of neutral C_{60} and both strong and weak DIBs (García-Hernández & Díaz-Luis 2013). In M 1-20, however, the final S/N (~ 20 at 4000 Å and >30 at wavelengths longer than 6000 Å) was not high enough to search the relatively broad (and weak) C_{60} features around 4000 Å or the weakest DIBs.

The optical spectroscopic observations of IC 418 (the brightest fullerene PNe in our sample) were carried out at the Nordic Optical Telescope (NOT; Roque de los Muchachos, La Palma) in March 2013 (under service time) with the FIES spectrograph. The optical spectra were taken in the wavelength range ~ 3600 – 7200 Å by using the FIES low-resolution mode (3630 – 7170 Å; orders 157–80) with the 2.5" fibre (centred at the IC 418 central star), which translates into a resolving power of $\sim 25,000$. Three exposures of 1200 s each were obtained in order to reach a S/N of ~ 60 at 4000 Å (and in excess of ~ 150 at wavelengths longer than 5000 Å) in the final combined IC 418 spectrum.

As comparison stars, for Tc 1 and M 1-20 we selected the nearby B-type stars HR 6334 ($B=5.1$; $E(B-V)=0.42$; Wegner 2003) and HR 6716 ($B=5.7$; $E(B-V)=0.22$; Wegner 2003), respectively, while HR 1890 ($B=6.4$; $E(B-V)=0.08$; Wegner 2003) was selected for IC 418. These comparison stars were observed on the same dates as the PNe and with the same VLT/UVES and FIES set-ups. Two exposures of 300 s were enough to obtain a final S/N in excess of ~ 300 in the final combined spectra of the comparison stars. The observed UVES and FIES spectra - processed with the UVES data reduction pipeline (Ballester et al. 2000) and with the FIES reduction software (FIEStool³), respectively - were corrected for heliocentric motion and combined, and the stellar continuum for the three PNe was fitted by using standard astronomical tasks in IRAF⁴. Table 1 lists some observational parameters, such as galactic coordinates, colour excess, and radial velocity for the three fullerene PNe in our sample and their corresponding comparison stars.

³ See <http://www.not.iac.es/instruments/fies/fiestool/FIEStool-manual-1.0.pdf>

⁴ Image Reduction and Analysis Facility (IRAF) software is distributed by the National Optical Astronomy Observatories, which is operated by the Association of Universities for Research in Astronomy, Inc., under cooperative agreement with the National Science Foundation.

Table 1. Observational parameters of fullerene PNe and their comparison stars.

Object	l	b	E(B-V)	V_r	Ref ^a	Comparison star	l	b	E(B-V)	V_r	Ref ^a
Tc 1	345.2375	-08.8350	0.23	-94.0	1, 2, 7	HR 6334	350.829	4.285	0.42	7.0	6, 9
M 1-20	6.187	8.362	0.80	75.0	3, 4, 7	HR 6716	7.162	-0.034	0.22	4.2	6, 10
IC 418	215.212	-24.284	0.23	62.0	4, 5, 8	HR 1890	208.177	-18.957	0.08	29.5	6, 10
HD 204827 ^b	99.167	5.552	1.06	20.0	6, 11						

Notes.

^(a) References. (1) Williams et al. (2008); (2) Frew et al. (2013); (3) Wang & Liu (2007); (4) McNabb et al. (2013); (5) Pottasch et al. (2004); (6) Wegner (2003); (7) Beaulieu et al. (1999); (8) Wilson (1953); (9) Kharchenko et al. (2007); (10) Pourbaix et al. (2004); (11) Petrie & Pearce (1961). ^(b) The Hobbs et al. (2008) reddened star used as a reference for DIBs (see Section 3).

3. DIBs towards PNe

We followed the list of DIBs measured in the high-S/N HD 204287 spectrum (Hobbs et al. 2008) to search for them in the VLT/UVES spectra of Tc 1 and M 1-20, as well as in the NOT/FIES spectrum of IC 418.

Our list of DIBs in Tc 1, M 1-20, and IC 418 are displayed in Tables A.1, A.2, and A.3, respectively, where we give the measured central wavelength (λ_c), the full width at half maximum (FWHM) as defined in Hobbs et al. (2008), the equivalent width (EQW⁵), the S/N in the neighbouring continuum, and the normalized equivalent widths (EQW/E(B-V)). For comparison, we also list in Table A.3 the EQW/E(B-V) values measured in HD 204827 and field-reddened stars by Hobbs et al. (2008) and Luna et al. (2008), respectively. The DIB parameters were measured using standard tasks in IRAF with no assumption on the DIB profiles; the only exception was the 4428 Å DIB for which we assumed a Lorentzian profile (see, e.g., Snow et al. 2002). We also list these parameters for the various interstellar components in those DIBs that are clearly resolved (e.g., the 6196 and 6379 Å DIBs; Table A.1).

The Tc 1 optical spectrum displays two interstellar clouds at -6.80 km s^{-1} and $+25.00 \text{ km s}^{-1}$, as indicated by the two absorption components for the atomic (Na I, Ca I) and molecular (CH⁺) lines (see Figures 1 and 2, Table A.4). Even the narrower DIBs towards Tc 1 (as 6379 Å) show this behaviour (see Figure 2 and Table A.4). The same behaviour is shown by the comparison star HR 6334, which also shows the two interstellar components at the same radial velocities as Tc 1, confirming that both stars map similar ISM conditions.

The M 1-20 optical spectrum, however, displays one Na I interstellar component (i.e., at -6.54 km s^{-1}) with a blue asymmetry that corresponds to a weaker non-resolved Na I interstellar component. Both components for the atomic Na I (e.g., at -6.12 , and -26.43 km s^{-1}) interstellar lines are clearly resolved in the comparison star HR 6716 (see Figure 3 and Table A.5), with the peculiarity that the Na I lines are broader in M 1-20. Only the strongest Na I interstellar component seems to be resolved in the DIBs (see Figure 3). The presence of two clear (and narrower) interstellar components in the comparison star suggests that both stars could map slightly different ISM conditions. For M 1-20 and its comparison star, we list the DIB parameters for the entire interstellar absorption (with no assumption on the DIB profile; Table A.2).

The PN IC 418 seems to show also a main Na I interstellar component at a radial velocity of $+22.22 \text{ km s}^{-1}$ and a much weaker, not completely resolved component at $\sim +5 \text{ km s}^{-1}$ (see Figure 4 and Table A.6). Thus, the DIB parameters for IC

418 are representative of the most prominent interstellar component (Table A.3). In the comparison star HR 1890, two interstellar components for the atomic Na I (e.g., at $+5.42$ and $+23.75 \text{ km s}^{-1}$) are clearly resolved, suggesting that both stars could map slightly different ISM conditions. Anyway, we list the DIB parameters for the entire interstellar absorption in both stars. We note that HR 1890 displays a very low reddening of $E(B-V)=0.08$, and only the strongest DIBs are clearly detected.

We identified 20, 12, and 11 DIBs in Tc 1, M 1-20, and IC 418, respectively. All of these absorption bands are known DIBs, as previously reported by Hobbs et al. (2008). It should be noted here that we could not estimate the total absorption of the well studied 6993 and 7223 Å DIBs in our three PNe because of the strong meddling from the telluric lines. We also note that our radial velocity analysis in Tc 1 shows that the ~ 6309 and 6525 Å absorption features reported by García-Hernández & Díaz-Luis (2013) should be identified as stellar He II absorption lines⁶. Their relative strengths (and widths) are consistent with the series of He II features that are clearly seen in our Tc 1 optical spectrum (e.g., at 6171, 6234, 6406, 6683, 6891, 7178, 8237, and 9345 Å).

3.1. Normal DIBs

We concentrate here on those DIBs that seem to be normal for their reddening, the so-called “normal” DIBs. In Tc 1, the PN with the highest quality spectrum and a proper comparison star, their strengths are consistent with the $E(B-V)$ value, and both PN and its comparison star display similar normalized equivalent widths (see Table A.1 and Figure 2). There are fifteen normal DIBs in Tc 1: six of them are among the strongest DIBs most commonly found in the ISM (5797, 5850, 6196, 6270, 6379, and 6614 Å)⁷, while the other nine DIBs (5776, 6250, 6376, 6597, 6661, 6792, 7828, 7833, and 8038 Å) are weaker interstellar features already reported by Hobbs et al. (2008). The situation is less clear for the fullerene PNe M 1-20 and IC 418. This is because the comparison stars for both PNe seem to map slightly different ISM conditions (see above). The comparison star of IC 418 also displays a very low reddening that prevents detection of a significant number of DIBs. Despite this, the classification of the latter DIBs (if detected in our spectra) as “normal” DIBs holds here for M 1-20 and IC 418 (see below).

⁶ These are the ~ 6310 and ~ 6527 Å stellar He II absorption lines, which are blue-shifted by $\sim 90 \text{ km s}^{-1}$ (the central’s star velocity) in Tc 1.

⁷ The parameters for the 5797 and 5850 Å DIBs are more uncertain in Tc 1 because of their low intrinsic intensity and some contamination by nearby spectral features. For example, there is a strong stellar absorption line of C IV at 5799.84 Å and a nebular emission feature in the proximity of the 5850 Å DIB.

⁵ One-sigma detection limits for the EQWs in our spectra scale as $\sim 1.064 \times \text{FWHM} / (S/N)$ (see, e.g., Hobbs et al. 2008).

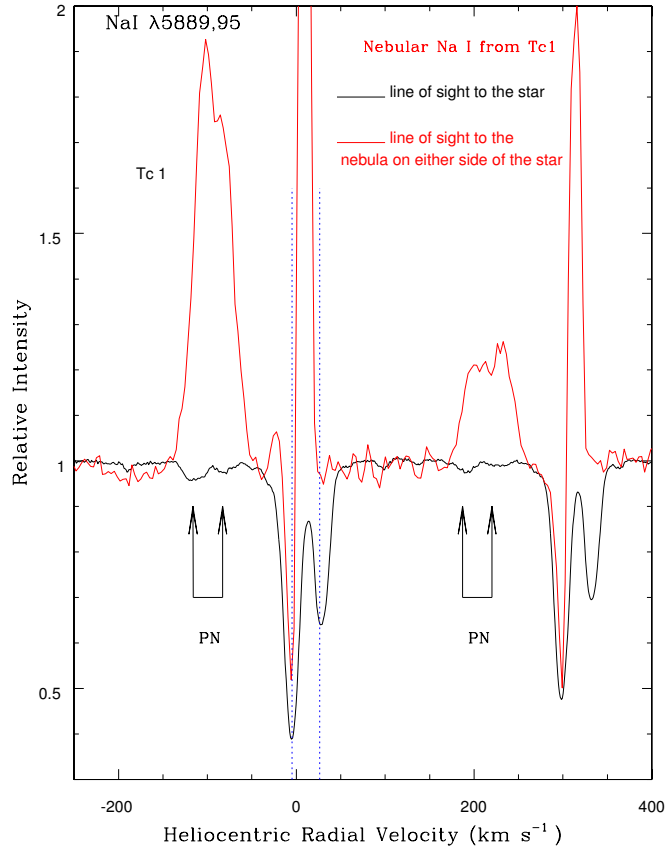


Fig. 1. Na I D lines observed towards PN Tc 1 central star (black) and average of two positions in the nebula 2.7 arcsec away from the central star on either side (red) (from Williams et al. 2008). The dashed blue lines indicate the interstellar Na I D components at -6.8 and $+25$ km s^{-1} . The sharp emission close to 0 km s^{-1} radial velocity is earth’s airglow. The absorption spectrum is in the stellar continuum units, while the emission spectrum is in the nebular continuum units.

The strengths of the sextet of common DIBs (5797 , 5850 , 6196 , 6270 , 6379 , and 6614 Å) are roughly consistent with the interstellar reddening in our three PNe. The EQW/E(B-V) ratio of these DIBs for the three PNe agree reasonably well with the values measured in their corresponding comparison stars (Tables A.1-3) or with the EQW/E(B-V) values observed in HD 204827 (Hobbs et al. 2008) and/or field-reddened stars (Luna et al. 2008). The 6196 , 6376 , 6379 , and 6661 Å DIBs towards Tc 1 (and its comparison star HR 6334) display the two interstellar components at the same radial velocities in both objects (Table A.1 and Figure 2). In M 1-20 and its comparison star HR 6716, we could measure only one main interstellar component for all DIBs (Table A.2 and Figure 3). As in the case of M 1-20, all common DIBs towards IC 418 (and its comparison star HR 1890) only display one main interstellar component (Table A.3 and Figure 4). We note, however, that only a few DIBs (five) are detected towards HR 1890 (Table A.3), and all DIBs are intrinsically very weak due to the very low reddening ($E(B-V)=0.08$) in the HR 1890 line of sight. Thus, Table A.3 also lists the EQW/E(B-V) values of HD 204827 (Hobbs et al. 2008) and field-reddened stars (Luna et al. 2008) for comparison with IC 418. The EQW/E(B-V) values of the sextet of common DIBs in IC 418 are similar to those in HD 204827 and field-reddened stars.

The measured intensities of the nine other “normal” DIBs (at ~ 5776 , 6250 , 6376 , 6597 , 6661 , 6792 , 7828 , 7833 , and 8038

Å)⁸ are also roughly consistent with the E(B-V) values in our three fullerene PNe. All these DIBs are detected in Tc 1. For the narrower 6196 , 6376 , 6379 , and 6661 Å DIBs in Tc 1 and its comparison star, we also give the parameters for each one of the interstellar components mentioned above (Table A.1). In M 1-20, however, only two (6376 and 6661 Å) of these weak DIBs are detected in our spectrum (Table A.2). In IC 418, we only detect the weak DIB at 6376 Å because the other weak DIBs are below our $1-\sigma$ detection limits.

In short, the carriers of the so-called “normal” DIBs do not seem to be particularly over-abundant towards fullerene PNe, since they are consistent with those expected for the general diffuse ISM.

3.2. Unusually strong DIBs

Interestingly, some DIBs are found to be unusually strong in fullerene PNe. The five DIBs at ~ 4428 , 5780 , 6203 , 6284 , and 8621 Å are unusually strong towards Tc 1. Their strengths in Tc 1 are higher than expected for the E(B-V) of 0.23 ; Tc 1 displays EQW/E(B-V) values higher than those in the comparison star HR 6334 (Table A.1 and Figure 2). This is clearly shown in Figure 5, where we plot the EQW/E(B-V) values of DIBs in Tc 1 versus HR 6334 (left panel) and those in the reference star HD 204827 versus HR 6334 (right panel). The EQW/E(B-V) val-

⁸ The parameters for the 5776 Å DIB are uncertain in Tc 1 because of its low intrinsic intensity and contamination by a nearby nebular emission feature.

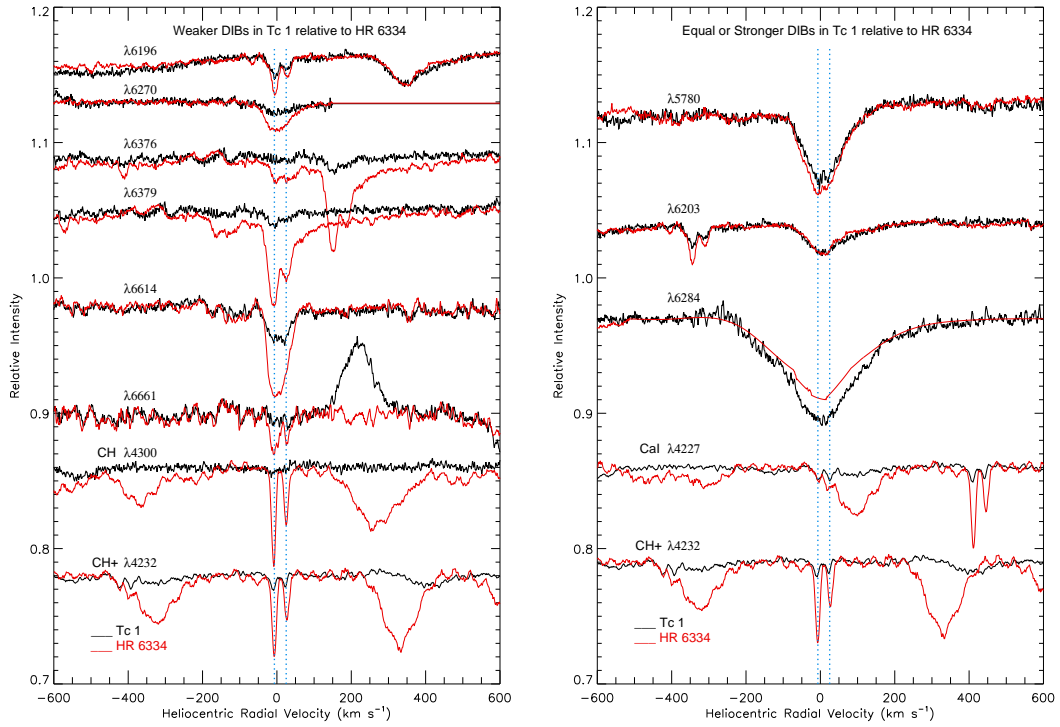


Fig. 2. Profiles of a selection of DIBs with various strengths and widths are displayed with respect to the heliocentric radial velocity. Weaker (or nearly equal) and stronger DIBs in Tc 1 (in black) relative to HR 6334 (in red) are displayed in the left and right panels, respectively. The profiles are shifted vertically for clarity. The CH, CH⁺, and Ca I profiles at the bottom show the two interstellar components at -6.8 and $+25$ km s⁻¹ (marked with blue vertical dotted lines) seen in both sources. The sharper DIBs in both Tc 1 and HR 6334 also show these two components. The DIBs displayed in the left panel are consistent with the lower reddening of $E(B-V)=0.23$ for Tc 1 as compared to $E(B-V)=0.42$ for HR 6334. The right panel, however, shows that the carrier(s) of these DIBs are enhanced (for the given $E(B-V)$) in the sight line to Tc 1.

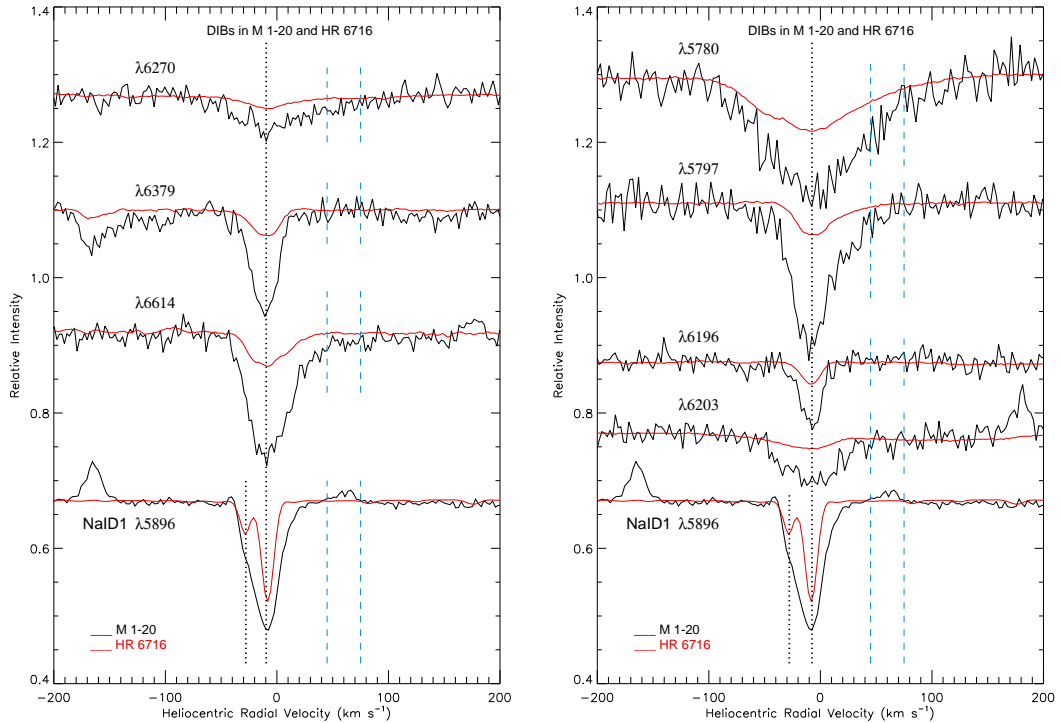


Fig. 3. Profiles of a selection of DIBs with various strengths and widths with respect to the heliocentric radial velocity. DIBs with similar and different profiles in M 1-20 (in black) relative to HR 6716 (in red) are displayed in the left and right panels, respectively. The profiles are shifted vertically for clarity. The Na I profiles at the bottom show the interstellar components (marked with black vertical lines) seen in M 1-20 and HR 6716. The DIBs displayed in the two panels are consistent with the higher reddening of $E(B-V)=0.80$ for M 1-20 as compared to $E(B-V)=0.22$ for HR 6716. The stellar (and nebular) radial velocity range for M 1-20 is denoted by blue vertical lines.

ues of DIBs in HR 6334 scale nicely with those in HD 204827 (the only exception is the 6284 Å DIB), suggesting similar ISM properties towards both stars. In Tc 1, however, the five unusually strong DIBs mentioned above clearly deviate from the linear relation followed by most of the DIBs that also scale well with those in HR 6334 (and HD 204827). The central radial velocity of these unusually strong interstellar features is the same in both Tc 1 and the comparison star (with the apparent exception of the 4428 Å feature; see Section 4), confirming their interstellar origin. In addition, the neutral molecular lines (CH, CN) are much weaker or absent towards Tc 1 (Figure 2), indicating a higher degree of ionization. This may indicate that carriers of these DIBs (enhanced towards Tc 1) may be ionized species.

The situation is again less clear for the fullerene PNe M 1-20 and IC 418. It seems clear, however, that at least the ~4428 Å DIB is unusually strong in both PNe (see below), showing EQWs that are much higher than expected for their E(B-V) values.

For the well-studied 4428 Å DB we adopted a Lorentzian profile (Snow et al. 2002), obtaining EQWs of ~860, 2579, and 1001 mÅ for Tc 1, M 1-20, and IC 418, respectively. The 4428 Å DB in Tc 1 and IC 418 is at least a factor of two greater than expected for their low reddening of E(B-V)=0.23 (see e.g., Fig. 6 and 15 in Snow et al. 2002 and van Loon et al. 2013, respectively), while this DB is ~1.5 times more intense than expected in M 1-20.

The DIB at 5780 Å is another interesting feature that also could be an unusually strong DIB towards IC 418 (Table A.3). In IC 418, it is stronger (EQW/E(B-V)=0.43) than in the comparison star HR 1890 (with EQW/E(B-V)=0.32) and in the Hobbs et al. (2008) reference star HD 294827. However, it has a similar strength to field-reddened stars (Luna et al. 2008). Unfortunately, the DIBs at ~6203 and 6284 Å are not present in the low-reddening star HR 1890. Similar to the 5780 Å DIB, these DIBs in IC 418 are stronger than in the star HD 294827 but of similar strength to those seen in the sample of field-reddened stars by Luna et al. (2008). Finally, our IC 418 optical spectra do not cover the spectral region around the 8621 Å feature.

As mentioned above, the situation is less clear also for M 1-20. Indeed, the 5780 and 6284 Å DIBs in M 1-20 are weaker than in HR 6716, while the 6203 Å DIB is of equal strength in both sources. Apparently, the bands at 5780, 6203, and 6284 Å seem to be unusually strong towards both M 1-20 and HR 6716 (see Table A2). As in the case of IC 418, these DIBs are stronger than in the reference star HD 294827 but similar to field-reddened stars. The most remarkable outcome is the complete lack of the 8621 Å DIB towards M 1-20, which otherwise is very intense in the Tc 1 line of sight.

Finally, it is worth mentioning here that the DIB at ~6203 Å varies among the fullerene PNe in our sample. This DIB and the other band at 6205 Å are usually measured as two distinct interstellar absorptions (e.g., corresponding to different carriers; see, e.g., Porceddu et al. 1991). The complex band at ~6203 Å is especially noteworthy, in which the EQW/E(B-V) ratio is two to three times higher for Tc 1 than for the comparison star HR 6334 and the reddened star HD 204827 (Hobbs et al. 2008). Towards IC 418, the 6203 Å DIB is not very strong, although is not detected in the line of sight of the low-reddening comparison star HR 1890. The 6203 Å DIB towards M 1-20 and its comparison star HR 6716 displays a similar EQW/E(B-V) ratio. Curiously, the secondary DIB at ~6205 Å is not clearly detected towards any of our sample PNe. This DIB is not easily recog-

nized (resolved) from the dominant 6203 Å DIB. Furthermore, we can find no evidence for the presence of the 6205 Å interstellar absorption in IC 418 because it coincides with a strong nebular emission line.

4. A search for diffuse circumstellar bands

The detection of diffuse circumstellar bands (DCBs) is very difficult because high S/N spectra are mandatory for detecting the presumably much weaker circumstellar features. Also, the DCBs have to be distinguished from the DIBs, and this distinction can only be made by measuring the radial velocities of the circumstellar and interstellar components in the line of sight to our PNe. The S/N is too low in PN M 1-20, preventing any search for DCBs towards this object. A higher quality (S/N~100-200) optical spectrum was obtained for IC 418, but its relatively low radial velocity (~58 km s⁻¹; Dinerstein et al. 1995) makes it difficult to distinguish possible DCBs from the DIBs. However, our high-quality (S/N > 300) spectra for PN Tc 1, together with its higher radial velocity (in the range from -83 to -130 km s⁻¹; Williams et al. 2008), may permit us to search for the possible presence of DCBs.

The nebular absorption lines in the line of sight to Tc 1 show heliocentric radial velocities in the range of -83 to -130 km s⁻¹ (Williams et al. 2008), while the star's heliocentric radial velocity is measured as -90±12 km s⁻¹. Any absorption/emission feature in the radial velocity range from -80 to -130 km s⁻¹ is then expected to be related to the Tc 1's expanding circumstellar (nebular) gas. Indeed, the Na I D lines show two distinct absorption components at -83 and -116 km s⁻¹ apart from the ISM components (see Figure 1 and Table A.4). The 5780 Å DIB towards Tc 1 matches the velocity of the ISM, as expected (see Figure 8). However, we find a (blue-shifted) very weak absorption feature (at the ~3-sigma level; EQW~6.8 mÅ and FWHM~0.99 Å) at the Tc 1 nebular velocity (centred at ~-125 km s⁻¹ and indicated in Figure 8), which is not present in the comparison star HR 6334 (see Figure 2). There is no known DIB at this wavelength, and it does not correspond to any stellar line (too narrow) or telluric feature (not present in HR 6334). In addition, the velocity separation is not in the right direction for another ISM cloud. This circumstellar absorption feature is narrower than the interstellar one, and the primary interstellar feature is broader owing to the contribution of at least two interstellar clouds (see above). The physical/chemical conditions in the Tc 1's circumstellar envelope are also expected to be different from those in the ISM, and the widths may not be necessarily the same. We note that there is a nebular emission counterpart (Figure 8) of the very weak DCB around 5780 Å, and the presence of this nebular emission at the radial velocity of Tc 1 furthermore suggests its circumstellar origin (see below).

Curiously, the 4428 Å feature in Tc 1 seems to be blue-shifted (by ~126 km s⁻¹) relative to the one in HR 6334 (see Figure 6). At the top of Figure 6, the profiles of Tc 1 have been shifted by 126 km s⁻¹ redwards and superposed on the HR 6334 profile to show the apparent difference in the profiles minima in both stars. It also aligns the photospheric lines of both stars, suggesting that the velocity of the 4428 Å absorption feature is close to the Tc 1's nebular velocity. In Figure 7, the profiles (normalized on the EQW of the 4428 Å band) of Tc 1 (left panel) and HR 6334 (right panel) have been superposed on the profile of an O6.5 star (HD 148937). This O6.5 star has been displaced (in velocity) in both panels to match the 4428 Å profiles observed in both Tc 1 and HR 6334. The 4428 Å profiles both in Tc 1

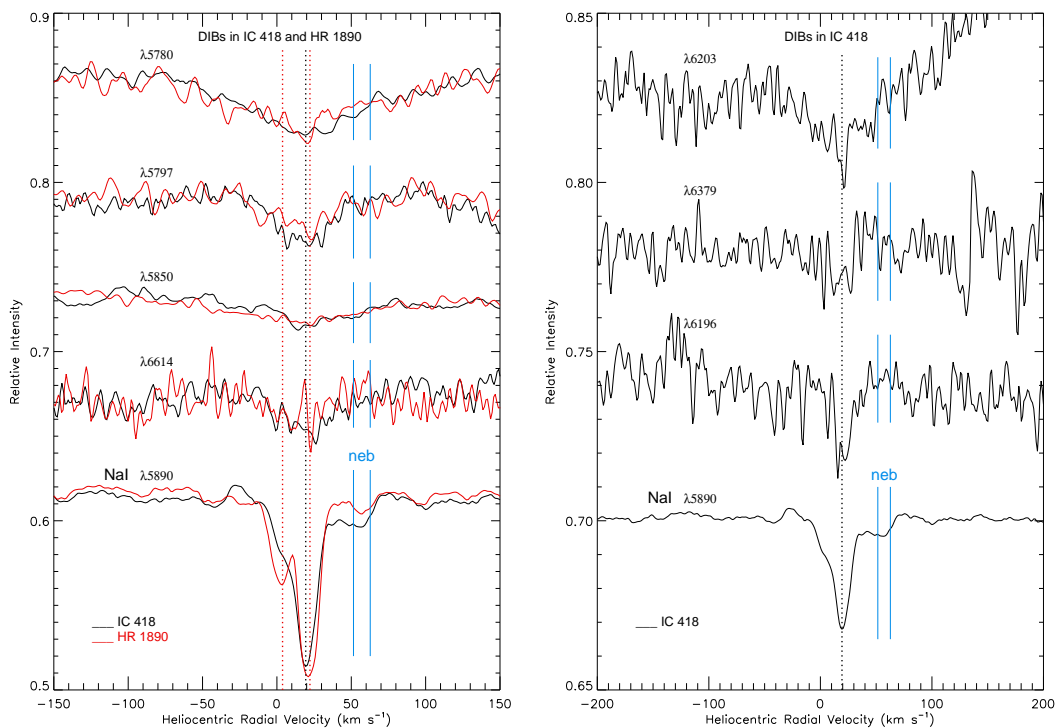


Fig. 4. Profiles of a selection of DIBs with various strengths and widths are displayed with respect to the heliocentric radial velocity. Some normal and unusually strong DIBs in IC 418 are displayed (not in HR 1890 due to the low reddening of 0.08). The Na I profiles show the prominent component at 22.22 km s^{-1} (marked with a black vertical dotted line) in IC 418.

and HR 6334 match the one in the O6.5 star (HD 148937) as well as our polynomial fits (the green profiles in Figure 7)⁹ This indicates that the minima of the 4428 \AA feature in Tc 1 and HR 6334 are well determined. The minimum of the 4428 \AA feature in HR 6334 occurs around 0.0 km s^{-1} , while it is blue-shifted by $\sim 126 \text{ km s}^{-1}$ in Tc 1. The blue shift could either be a result of vibrational-rotational structure of the carrier molecule or could be due to radial motions of the carriers. The velocity shift is about the same amount as the radial velocity of the circumstellar gas of Tc 1 (also the Na I D absorption components). A nebular emission feature is present at the wavelength corresponding to the blue shift of $\lambda 4428$ absorption feature (see below), which cannot be identified with any nebular line (see, e.g., Sharpee et al. 2003 for a complete compilation of nebular lines in PN IC 418 that displays an effective temperature that is almost identical to Tc 1). Thus, it seems likely that the apparent blue shift of the 4428 \AA feature is real, indicating a circumstellar (nebular) nature for the carrier(s). Also, the ISM contribution to the 4428 \AA feature in Tc 1 is expected to be a minor one; even smaller than the one in HR 6334.

If the material in and around the nebula (plus central star) is giving rise to the circumstellar absorption components in the sight line towards the star (as seen in Na I D and some DIBs), then the same material is expected to be seen in emission in the sight lines of the nebula away from the central star. We have investigated the Tc 1 nebular spectra obtained by Williams et al. (2008) and their spectroscopic observations in sight lines away from the central star indeed seem to confirm this expectation. The average spectrum of the nebula at two slit positions 2.7 arc

sec away from the Tc 1 central star (Williams et al. 2008) - which samples the same *Spitzer* volume that revealed the fullerenes in Tc 1 - shows the Na I D lines in emission (also the Ca II K lines, but these are much weaker) at the radial velocity of the object (see Figure 1 and Table A.1). The Na I D emission components have slightly more positive radial velocity ($\sim 10 \text{ km s}^{-1}$ with respect to the absorption lines), suggesting a possible expansion velocity of -10 km s^{-1} for the Na I gas. Such a correspondence of emission feature occurs with $\lambda 4428$ absorption. Similar emission corresponding to $\lambda 5780$ also seems to be present in the Tc 1 nebular spectrum. The presence of 4428 and 5780 \AA nebular emission (see Figure 8) at the radial velocity of Tc 1 furthermore suggests their circumstellar origin. The DCBs reported here are known to be among the strongest DIBs. The strong 4428 \AA feature is known to correlate well with other DIBs like 5780 (e.g., van Loon et al. 2013). The 5780 \AA DIB is also known to correlate with the broad 6284 \AA feature in the ISM (see, e.g., Friedman et al. 2011) but might differ in circumstellar environments. Interestingly, the 6284 \AA DIB is very strong in Tc 1 and might even be hiding a circumstellar absorption feature as well; in Figure 2, there is evidence of some asymmetry in the 6284 \AA DIB profile at the Tc 1's radial velocity range (from -83 to -130 km s^{-1}).

The PN IC 418 also shows circumstellar (nebular) absorption components (although much weaker than in Tc 1) in the Na I D lines (Dinerstein et al. 1995; see also Figure 4 and Table A.6). Indeed, the 5780 \AA DIB towards IC 418 displays a tentative weak asymmetry (even weaker than towards Tc 1) at the nebular velocity of $\sim 58 \text{ km s}^{-1}$. Unfortunately, the 4428 \AA feature is not seen in its (low reddening) comparison star HR 1890, and we could not properly check whether the profile minimum of this feature is red-shifted to the observed nebular velocity of

⁹ Despite the pollution by many lines in HR 6334, Figure 7 shows that the 4428 \AA profile in HR 6334 match our polynomial fit very well (the green profile in Figure 7 (right panel)).

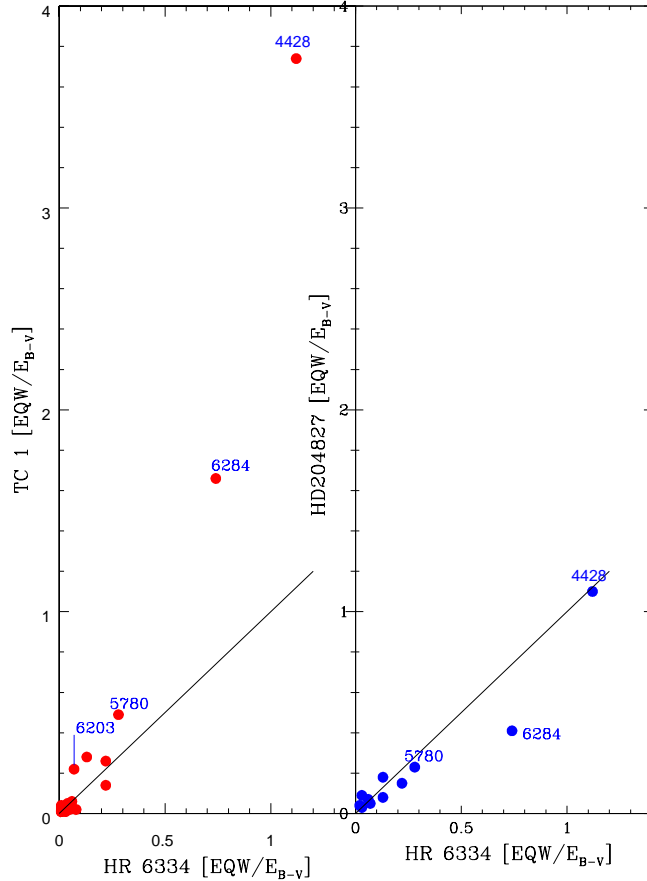


Fig. 5. Plots of EQW/E(B-V) of Tc 1 with respect to (w.r.t.) HR 6334 (left panel) and HD 204827 w.r.t. HR 6334 (right panel). The EQW/E(B-V) values of HR 6334 scale nicely w.r.t. HD 204827, which suggests that the properties of ISM are similar for DIBs towards the two stars. For Tc 1, most of the DIBs also scale well w.r.t. HR 6334 (and HD 204827) with the exception of the five unusually strong DIBs (those at ~ 4428 , 5780, 6203, 6284, and 8621 Å; see text), which deviate from the linear relation.

IC 418. The comparison of the 4428 Å profile in IC 418 with the one in the O6.5 star HD 148937 displayed in Figure 9 tentatively suggests that this feature in IC 418 could be slightly red-shifted with respect to the expected interstellar wavelength. However, the 4428 Å profile in IC 418 is not fully reproduced by the one in HD 148937, and the central wavelength of this feature is uncertain (i.e., more uncertain than in the case of Tc 1 above).

As mentioned above, the S/N in the M 1-20 spectrum is probably too low for detecting DCBs in this object. The heliocentric radial velocity of the nebula has been measured by us as ~ 61 km s $^{-1}$ (from a few He I nebular emission lines). This radial velocity is shown in Figure 3. In our low S/N M 1-20 spectrum, there is no evidence of any DIB component close to this radial velocity.

Based on the EQW of the strong DIB at 5780 Å towards Tc 1 (EQW=112.1 mÅ) relative to the weak DCB around the same wavelength (EQW=6.8 mÅ), we can estimate the S/N needed to detect this DCB in M 1-20 and IC 418. An EQW(DIB)/EQW(DCB) ratio of 16.5 is obtained for Tc 1. Adopting this value for the other PNe, one can estimate the expected EQW of the 5780 Å DCB; EQW(DCB) values of 20.1, and 6.1 mÅ are obtained for M 1-20 and IC 418, respectively. Then, when assuming the same FWHM (990 mÅ) as in Tc 1, the needed S/N for the DCB feature to be detected at three sigma can be obtained (EQW $\sim 3 \times$ FWHM / (S/N); see Hobbs et al. 2008). We find that we would need S/N ~ 143 and 491 for M 1-20 and

IC 418, respectively. Thus, our non-detection of the DCBs in the latter PNe is due to the lower S/N in our spectra for both objects (see Tables A.2 and A.3).

In summary, the present data show that DCBs might not be uncommon in fullerene-containing PNe and suggest the first detection of two DCBs at 4428 and 5780 Å in the fullerene-rich circumstellar environment around the PN Tc 1. However, we prefer to be cautious until these possible DCB detections are confirmed in other PNe with fullerenes. The three fullerene-containing PNe in our sample display very weak circumstellar absorptions of Na I, and the intrinsic weakness of the DCBs (e.g., 5780 Å) is very likely related with the low column density of the gas (and dust) in their circumstellar envelopes. The strength of the 5780 Å circumstellar absorption in fullerene PNe is likely to be correlated with the circumstellar Na column density and the best PNe to unambiguously confirm that our detection of DCBs are those showing a strong Na I circumstellar absorption that is well separated (i.e., at a very different radial velocity) from the Na I interstellar components.

5. Electronic transitions of neutral C₆₀ in fullerene PNe

The strongest allowed electronic transitions of neutral gas phase C₆₀ molecules, as measured in laboratory experiments, are located at 3760, 3980, and 4024 Å with widths of 8, 6, and 4 Å,

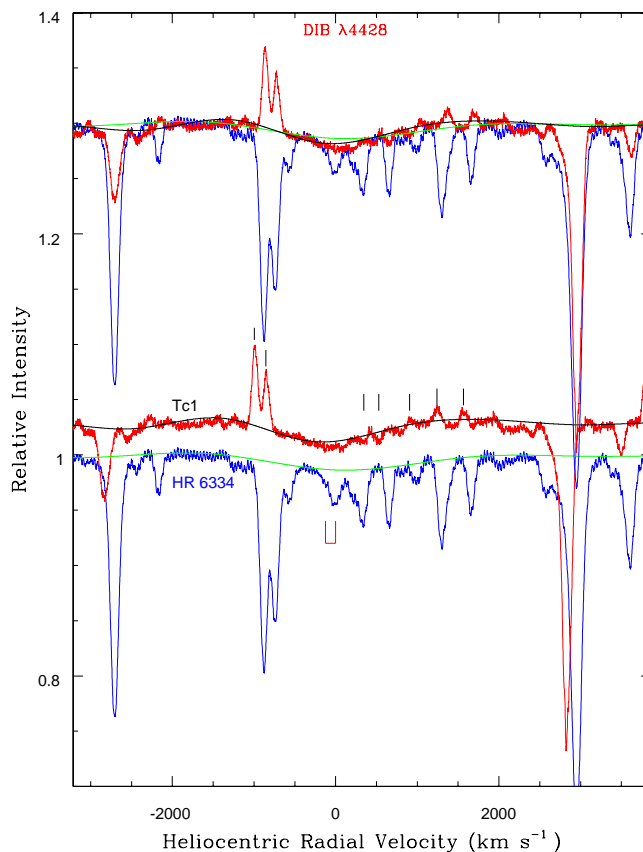


Fig. 6. Profiles of the 4428 Å feature in Tc 1 (red) and in the comparison star HR 6334 (blue). The black and green profiles of the 4428 Å feature have been constructed by avoiding the stellar emission and absorption lines (marked by short black lines) and by fitting a high-degree polynomial function to the clearer regions. The minimum of the 4428 Å feature in HR 6334 occurs around 0.0 km s⁻¹, while it seems to be blue-shifted in Tc 1. At the top, the profiles of Tc 1 has been shifted by 126 km s⁻¹ redwards and superposed on the HR 6334 profile to illustrate the apparent non-coincidence of the minima of the profiles in both stars.

respectively (Sassara et al. 2001; see also García-Hernández et al. 2012b). García-Hernández & Díaz-Luis (2013) found no evidence of these strong neutral C₆₀ optical bands in absorption (or emission) in the fullerene PN Tc 1.

The S/N in the M 1-20 optical spectrum is too low to search for neutral C₆₀ features in its spectrum (García-Hernández & Díaz-Luis 2013), but here we have searched the higher S/N (~100 in the continuum around 4000 Å) spectrum of the PN IC 418 for the strongest electronic transitions of neutral C₆₀ mentioned above. As in the case of Tc 1, we can find no evidence of neutral C₆₀ in absorption (or emission) around the expected wavelengths of ~3760, 3980, and 4024 Å. This is shown in Figure 10 where we display the IC 418 velocity-corrected spectra around the most intense C₆₀ transitions in comparison with those of Tc 1 and its comparison star HR 6334. We note that several strong O lines and He I 4026 Å very likely prevent identification of any broad and weak absorption feature around 3760 and 4024 Å, respectively. However, there is no evidence of the neutral C₆₀ feature at 3980 Å, a wavelength region that is free of other spectral features.

The one-sigma detection limits on the EQWs derived from our IC 418 spectrum are 202, 75, and 44 mÅ for the 3760, 3980, and 4024 Å neutral C₆₀ transitions, respectively. By using the Spitzer formula ($N \sim 10^{20} \times (\text{EQW}/(\lambda^2 \times f))$), where f is the oscillator strength of each C₆₀ transition (Sassara et al. 2001), this

translates into column densities of $\sim 2 \times 10^{13}$, 4×10^{13} , and 2×10^{13} cm⁻². These column density limits are similar to those previously obtained in Tc 1 by García-Hernández & Díaz-Luis (2013). By following the latter work, we could in principle compare these column-density limits with estimates of the circumstellar density of C₆₀ molecules as derived from the IR C₆₀ emission bands.

Unfortunately, only two C₆₀ IR bands (those at ~17.4 and 18.9 μm) were covered by the IC 418 *Spitzer* spectrum, making the estimation of the number of C₆₀ molecules ($N(\text{C}_{60})$) and excitation temperature ($T(\text{C}_{60})$) from the Boltzmann excitation diagram rather uncertain. Such column-density estimates are very sensitive to $T(\text{C}_{60})$, and this temperature is very poorly constrained in IC 418 given that the short wavelength C₆₀ bands are not available and that the C₆₀ 17.4 μm band is blended with PAH emission. In addition, the derivation of the C₆₀ column density based on the IR-emission spectrum relies on the assumption that C₆₀ is at thermal equilibrium, and this is still an open question (see, e.g., Bernard-Salas et al. 2012).

6. A fullerene - diffuse band connection?

Most of the strongest and well-studied DIBs, as well as other weaker DIBs towards Tc 1, are found to be normal for its reddening. This indicates that the carriers of these “normal” DIBs are not particularly overabundant towards fullerene PNe. The

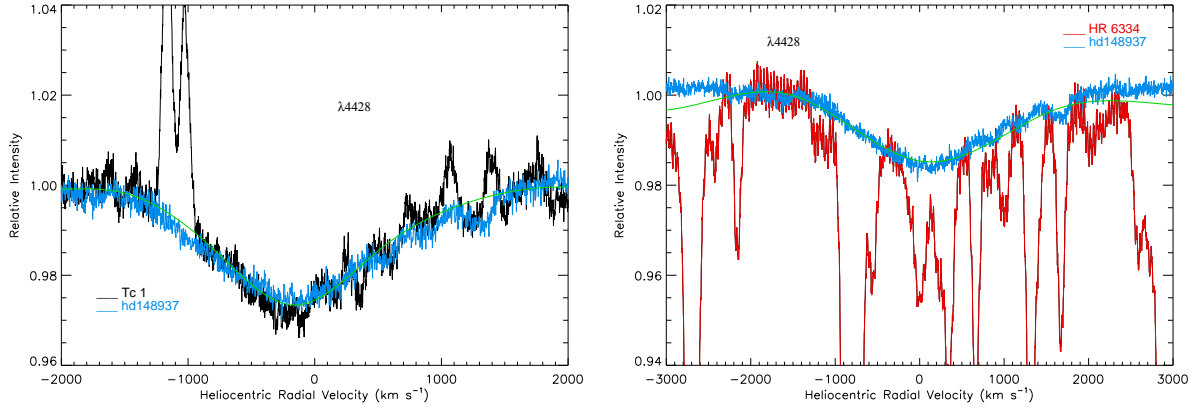


Fig. 7. Profiles of the 4428 Å feature in Tc 1 (left panel) and in the comparison star HR 6334 (right panel) superposed on the profile of the O6.5 star HD 148937. The O6.5 star has been displaced (in velocity) in both panels to make the 4428 Å band coincide with the profile and the minima of the 4428 Å band towards Tc 1 and HR 6334. All spectra have been normalized on the EQW of the 4428 Å band. The minimum of the feature in HR 6334 occurs around 0.0 km s⁻¹, while it seems to be blue-shifted in Tc 1. The green profiles of the 4428 Å feature in Tc 1 and HR 6334 are the polynomial fits shown in Figure 6. The superposed spectrum of an O6.5 star (in blue) support the non-coincidence of the profiles minima in Tc 1 and HR 6334.

exceptions are the DIBs at 4428, 5780, 6203, 6284, and 8621 Å, which are found to be unusually strong towards Tc 1. The radial velocities of the 5780, 6203, 6284, and 8621 Å features confirm their interstellar origin, and the higher degree of ionization towards Tc 1 (in comparison with its comparison star) suggests that their carriers may be ionized species. The 4428 Å feature, however, seems to be centred at the Tc 1's radial velocity, suggesting a circumstellar origin (see Section 4). The situation is less clear for M 1-20 and IC 418 because their comparison stars seem to map slightly different ISM conditions (see Section 3.2), but at least the 4428 Å feature is also found to be unusually strong in the latter fullerene PNe.

The unusually strong 4428 Å feature towards Tc 1 and M 1-20 prompted the idea that the 4428 Å carrier may be related to fullerenes or fullerene-based molecules (García-Hernández & Díaz-Luis 2013). Our new finding of an unusually strong 4428 Å feature towards IC 418 suggests that this may be a common characteristic of fullerene PNe, reinforcing the speculation of a possible fullerene-DIB connection.

Our detection of DCBs at 4428 and 5780 Å in an environment rich in fullerenes and fullerene-related molecules would inevitably provide a link between fullerene compounds and the DIB carriers. Photo-absorption theoretical models of several large fullerenes (such as C₈₀, C₂₄₀, C₃₂₀, and C₅₄₀) and multi-shell fullerenes (carbon onions like C₆₀@C₂₄₀, C₆₀@C₂₄₀@C₅₄₀) predict their strongest optical (4000–7000 Å) transitions very close to 4428 and 5780 Å (Iglesias-Groth 2007), suggesting they are possible carriers.

We can estimate abundances of the carriers of the DCBs at 4428 and 5780 Å in PN Tc 1. For a Tc 1 carbon abundance of 4.7×10^{-4} (relative to H; e.g., García-Hernández et al. 2012a), the fraction of elemental carbon (f_C) that is locked in the carrier molecule M can be expressed as (see, e.g., Tielens 2005; Cami 2014)

$$f_C \sim 9.93 \times 10^{-3} \times \frac{W_\lambda}{E_{B-V}} \times \frac{N_C}{60} \times \frac{5000^2}{\lambda^2} \times \frac{10^{-2}}{f}, \quad (1)$$

where W_λ/E_{B-V} is the equivalent width per reddening unit (in Å magnitude⁻¹), N_C is the number of carbon atoms, and λ

and f are the transition wavelength (in Å) and oscillator strength, respectively.

Assuming $f=0.01$ (Watson 1994; Weisman et al. 2003) and $N_C \geq 60$ (as appropriate for large fullerenes and buckyonions), we find the well known result that the 4428 and 5780 Å carriers have to be very abundant or else they have larger oscillator strengths (Tielens 2005). For example, $f_C \sim 0.06, 0.19,$ and 0.42 for C₈₀, C₂₄₀, and C₅₄₀, respectively, if these fullerene species are considered to be the only carrier of the 4428 Å feature¹⁰. In Tc 1, the fraction of elemental carbon that is locked in C₆₀ is estimated to be $\sim 4 \times 10^{-4}$ (as estimated from the IR emission; e.g., García-Hernández et al. 2012a). However, most fullerenes bigger than C₆₀ and multi-shell fullerenes (buckyonions) display strong transitions close to 4428 Å (Iglesias-Groth 2007). Thus, in the fullerene-DIB hypothesis, the broad 4428 Å feature would be the result of the superposition of the transitions of a series (family) of fullerenes bigger than C₆₀ and buckyonions, and each fullerene compound would contribute to the total EQW observed. Unfortunately, at present the possible relative contribution (e.g., in terms of FWHM and EQW) of these fullerene compounds to the 4428 Å feature is not known.

More interesting is that only C₅₄₀ and C₆₀@C₂₄₀@C₅₄₀ display a strong transition near 5780 Å (Iglesias-Groth 2007). By considering the latter fullerene species (and using $f=0.01$) as the only carrier of the 5780 Å feature, $f_C \sim 2 \times 10^{-3}$ and 3×10^{-3} are obtained for C₅₄₀ and C₆₀@C₂₄₀@C₅₄₀, respectively. Thus, a greater oscillator strength (e.g., $f=0.1$) for the C₅₄₀ and C₆₀@C₂₄₀@C₅₄₀ transitions at 5780 Å would decrease the latter estimates to levels similar to C₆₀. On the other hand, it is to be noted here that the C₆₀ abundance estimation in Tc 1 (e.g., García-Hernández et al. 2012a) assumes a uniform C₆₀ spatial distribution in the circumstellar shell. Bernard-Salas et al. (2012) present evidence that the C₆₀ emission in Tc 1 is extended and peaks far away from the central star. If the C₆₀ molecules in Tc 1 are indeed distributed in a ring (or in clumps) around the central star, then the quoted C₆₀ abundance of $\sim 4 \times 10^{-4}$ (relative to C; e.g., García-Hernández et al. 2012a) should be considered as a lower limit. This may increase the C₆₀ abundance

¹⁰ Similar values are obtained for the 4428 Å feature in the other fullerene PNe M 1-20 and IC 418.

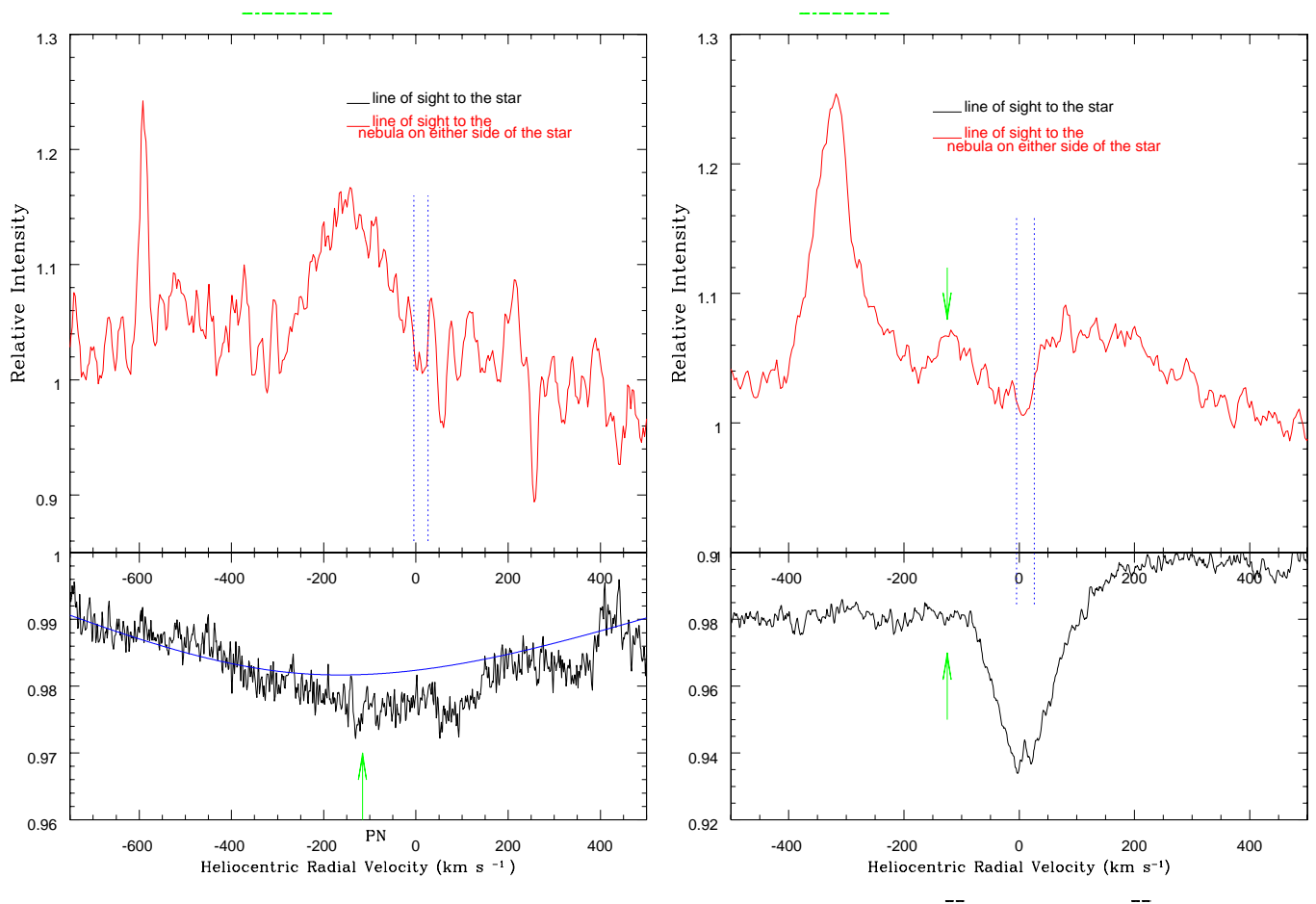


Fig. 8. Profiles of the broad 4428 Å band (left panel) and of the 5780 Å feature (right panel) towards Tc 1 central star (black) and average of two sight lines to the nebular position on either side of the nebula (from Williams et al. 2008). In both panels, the dashed blue lines mark the interstellar components at -6.8 and $+25$ km s⁻¹. Note the coincidence in velocity (marked by green arrows) of the profile centre of the broad 4428 Å and of the weak 5780 Å circumstellar absorptions and the corresponding nebular emissions. The emission feature to the left of the 5780 Å nebular emission is unidentified.

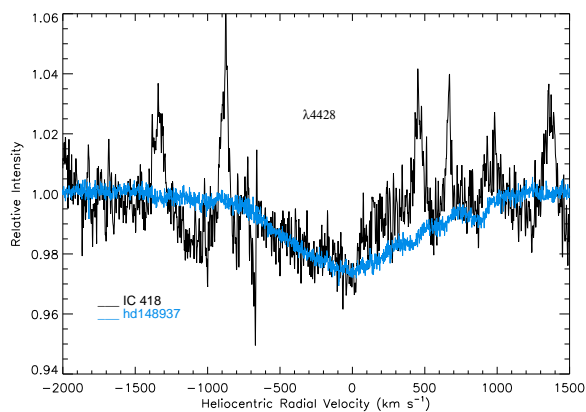


Fig. 9. Profiles of the 4428 Å feature in IC 418 (in black) superposed on the profile of the O6.5 star HD 148937 (in blue). The O6.5 star has been displaced (in velocity) to try the 4428 Å band coincide with the profile and the minima of the 4428 Å band towards IC 418. Note that both spectra have been normalized on the EQW of the 4428 Å band. The 4428 Å profile in IC 418 is not fully reproduced by that in HD 148937 and its central wavelength is quite uncertain (see text).

estimate (from the IR emission) in Tc 1 to values higher than the 5780 Å carrier/s abundance estimated here. In addition, it may explain the lack of the strongest optical electronic transitions of the C₆₀ molecule in Tc 1 (and IC 418).

From the previous paragraphs, we conclude that at present large fullerenes and buckyonions cannot be completely discarded as possible carriers of the 4428 Å and 5780 Å features. However, another fullerene-related species should be considered as possible diffuse band carriers (see below).

Recent experimental studies demonstrate that fullerenes (and metallofullerenes) would react with polycyclic carbon, graphene-like structures, and PAHs, forming a rich family of fullerene-based molecules such as fullerene/PAH clusters and endohedral metallofullerenes (Dunk et al. 2013). These fullerene-related species may still be excited by the UV photons from the central star, emitting through the same IR vibrational modes as empty cages. Laboratory work shows that fullerene/PAH adducts (such as C_{60} /anthracene) can easily form via Diels-Alder cyclo-addition reactions, displaying mid-IR features strikingly coincident with those from neutral C_{60} and C_{70} (García-Hernández, Cataldo & Manchado 2013). In addition, gas-phase reactions between PAHs and C_{60} and C_{70} are experimentally proven to occur under circumstellar/interstellar conditions (Dunk et al. 2013), and the resulting reaction products (e.g., C_{70} -PAH cluster ions like $C_{70}C_{24}H_{10}^+$) are very stable. Metals such as Na (and Ca) are also quite abundant in the fullerene-rich circumstellar envelope of Tc 1 and metallofullerene (e.g., $Na@C_{60}$) formation is expected to be as efficient as empty fullerenes (Dunk et al. 2013). Indeed, theoretical spectra of $Na@C_{60}$ (Dunk et al. 2013) show the same four vibrational modes as neutral C_{60} (but with much higher absorption intensities), together with a new IR-active vibrational mode due to the metal encapsulation. Interestingly, the wavelength position of this new mode is quite close to the still unidentified $\sim 6.4 \mu m$ feature observed in Tc 1 and other fullerene-rich PNe (Dunk et al. 2013; García-Hernández et al. 2010, 2011b, 2012a; Bernard-Salas et al. 2012).

Certainly, metallofullerenes are better diffuse band carrier candidates than fullerene/PAH adducts because the latter species are less stable towards UV radiation (see, e.g., Kroto & Jura 1992). In particular, adducts of C_{60} with linearly condensed PAHs (acenes such as anthracene, tetracene, and pentacene; e.g., García-Hernández, Cataldo & Manchado 2013) are not as stable as those with pericondensed PAHs (e.g., coronene); under the action of strong UV radiation (e.g., from the central star), the C_{60} /acene adducts may be dissociated back to the starting molecules. However, if the C_{60} /acene adducts are formed in a circumstellar region shielded from the UV radiation (or they are absorbed by dust particles), then they could survive in PNe circumstellar shells.

In short, fullerenes in their multifarious manifestations - buckyonions, fullerene clusters, fullerenes-PAHs, metallofullerenes, fullerene-like fragments or buckybowl structures - may help solve the long-standing astrophysical problem of the identification of some of the DIB carriers. Our detection of DCBs at 5780 and 4428 Å in Tc 1 may thus help to identify the carrier molecule(s), so more theoretical/laboratory work on fullerene-related molecules is encouraged.

7. Conclusions

We have searched DIBs in the optical spectra towards three fullerene-containing PNe (namely Tc 1, M 1-20, and IC 418). We have identified 20, 12, and 11 DIBs towards Tc 1, M 1-20, and IC 418, respectively. All of these absorption bands are known DIBs as previously reported in the literature.

Towards Tc 1, the PN with the highest S/N spectrum and a proper comparison star, six of the strongest and well-studied DIBs (i.e., those at 5797, 5850, 6196, 6270, 6379, and 6614 Å), and nine other weaker interstellar features (i.e., those at 5776, 6250, 6376, 6597, 6661, 6792, 7828, 7833, and 8038 Å) are found to be normal for its reddening. This indicates that the

carriers of these “normal” DIBs are not particularly overabundant towards fullerene PNe. The five DIBs at 4428, 5780, 6203, 6284, and 8621 Å are found to be unusually strong in the Tc 1 line of sight. The radial velocities of the 5780, 6203, 6284, and 8621 Å features confirm their interstellar origin, and the high ionization degree towards Tc 1 suggests that their carriers may be ionized species. The 4428 Å feature, however, seems to be centred at the Tc 1’s radial velocity, suggesting a circumstellar origin.

The situation is less clear for the fullerenes PNe M 1-20 and IC 418, because their spectra are of lower quality than in Tc 1, and their comparison stars seem to map slightly different ISM conditions. In spite of this, the same classification scheme (“normal” versus “unusually strong” DIBs) seems to be applicable towards M 1-20 and IC 418. At least the 4428 Å feature is found to be unusually strong in these objects, as a common characteristic to fullerene PNe.

The Tc 1’s high radial velocity permitted us to search its high-quality optical spectrum for DCBs. Interestingly, we report the first tentative detection of two DCBs at 4428 and 5780 Å in the fullerene-rich circumstellar environment around Tc 1. The presence of 4428 and 5780 Å nebular emission at the radial velocity of Tc 1 further suggests their circumstellar origin. The non-detection of DCBs in the other fullerene PNe is due to the low S/N in our optical spectra.

Moreover, we can find no evidence of the strongest electronic transitions of neutral C_{60} in the IC 418 optical spectrum. The non-detection of neutral C_{60} optical absorptions in fullerene PNe could be explained if the C_{60} IR emission peaks far away from the central star. Mid-IR images at high spatial resolution and centred on the C_{60} features would be desirable to understand the lack of the C_{60} optical bands in fullerene-containing PNe.

We have estimated the abundances of the carriers of the DCBs at 4428 and 5780 Å, and we conclude that at present large fullerenes and buckyonions cannot be completely discarded as possible carriers of the 4428 and 5780 Å features.

On the basis of detecting DCBs at 4428 and 5780 Å in Tc 1, we suggest that laboratory and theoretical studies of fullerenes in their multifarious manifestations - buckyonions, fullerene clusters, fullerenes-PAHs, metallofullerenes, fullerene-like fragments or buckybowl structures - may help solve the astronomical mystery of the identification of some of the DIB carriers.

Acknowledgements. We acknowledge the anonymous referee for very useful suggestions that helped to improve the paper. We also acknowledge Jack Baldwin, Robert Williams, and Mark Phillips for supplying us with the nebular spectrum of Tc 1, as well as Jorge García-Rojas for his help during the data analysis. N.K.R. thanks the Instituto de Astrofísica de Canarias for inviting him as a Severo Ochoa visitor during January to April 2014 when part of this work was done. J.J.D.L., D.A.G.H., and A.M. acknowledge support provided by the Spanish Ministry of Economy and Competitiveness (MINECO) under grant AYA-2011-27754. D. A. G. H. also acknowledges support provided by the MINECO grant AYA-2011-29060. This work is based on observations obtained with ESO/VLT under the programme 087.D-0189(A). This article is also partially based on service observations made with the Nordic Optical Telescope operated on the island of La Palma by the Nordic Optical Telescope Scientific Association in the Spanish Observatorio del Roque de Los Muchachos of the Instituto de Astrofísica de Canarias.

References

- Ballester, P., Modigliani, A., Boitquin, O. et al. 2000, *Messenger*, 101, 31
- Beaulieu, S. F., Dopita, M. A., & Freeman, K. C. 1999, *ApJ*, 515, 610
- Bernard-Salas, J., Cami, J., Peeters, E. et al. 2012, *ApJ*, 757, 41
- Berné, O., Mulas, G., & Joblin, C. 2013a, *A&A*, 550, L4

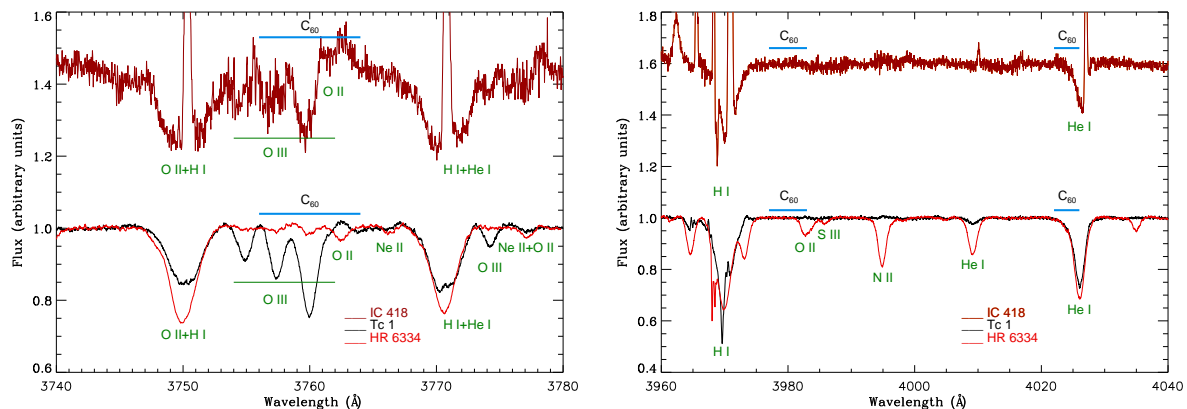


Fig. 10. Velocity-corrected spectra of IC 418 (in brown), Tc 1 (in black) and HR 6334 (in red) around 3760 Å (left panel) and 4000 Å (right panel) where the atomic line identifications are indicated (in green). The expected positions (and FWHMs) of the C_{60} features are indicated on top of the spectra. There is no evidence (additional absorption and/or emission) in IC 418 and Tc 1 for the neutral C_{60} features at 3760, 3980, and 4024 Å.

- [] Berné, O., Mulas, G., & Joblin, C. 2014, in *The Diffuse Interstellar Bands*, Proceedings of the International Astronomical Union, IAU Symposium, Volume 297, pp. 203-207
- [] Cami, J. et al. 2010, *Science*, 329, 1180
- [] Cami, J. 2014, in *The Diffuse Interstellar Bands*, Proceedings of the International Astronomical Union, IAU Symposium, Volume 297, pp. 370-374
- [] Cataldo, F., Strazzulla, G., & Iglesias-Groth, S. 2009, *MNRAS*, 394, 615
- [] Cox, N. L. J. 2011, in *PAHs and the Universe: A Symposium to Celebrate the 25th Anniversary of the PAH Hypothesis*, EAS Publication Series Vol. 46, 349-354, eds Joblin, C. & Tielens, A. G. G. M.
- [] Crawford, M. K., Tielens, A. G. G. M., & Allamandola, L. J. 1985, *ApJ*, 293, L45
- [] Dinerstein, H. L., Sneden, C., & Uglum, J. 1995, *ApJ*, 447, 262
- [] Dunk, P. W., Adjizian, J. J., Kaiser, N. K. et al. 2013, *PNAS*, 110 (45), 18081
- [] Foing, B. H., & Ehrenfreund, P. 1994, *Nature*, 369, 296
- [] Frew, D. J., Bojicic, I. S., & Parker, Q. A. 2013, *MNRAS*, 431, 2
- [] Friedman, S. D., York, D. G., McCall, B. J., et al. 2011, *ApJ*, 727, 33
- [] García-Hernández, D. A., Manchado, A., García-Lario, P. et al. 2010, *ApJ*, 724, L39
- [] García-Hernández, D. A., Iglesias-Groth, S., Acosta-Pulido, J. A. et al. 2011a, *ApJ*, 737, L30
- [] García-Hernández, D. A., Rao, N. K., & Lambert, D. L. 2011b, *ApJ*, 729, 126
- [] García-Hernández, D. A., Rao, N. K., & Lambert, D. L. 2011c, *ApJ*, 739, 37
- [] García-Hernández, D. A., Villaver, E., García-Lario, P. et al. 2012a, *ApJ*, 760, 107
- [] García-Hernández, D. A., Rao, N. K., & Lambert, D. L. 2012b, *ApJ*, 759, L21
- [] García-Hernández, D. A., Cataldo, F., & Manchado, A. 2013, *MNRAS*, 434, 415
- [] García-Hernández, D. A., & Díaz-Luis, J. J. 2013, *A&A*, 550, L6
- [] Geballe, T. R., Najjarro, F., Figer, D. F. et al. 2011, *Nature*, 479, 200
- [] Heger, M. L. 1922, *Lick Obs. Bull.* 10, 146
- [] Herbig, G. H. 1993, *ApJ*, 407, 142
- [] Hobbs, L. M., York, D. G., Snow, T. P. et al. 2008, *ApJ*, 680, 1256
- [] Iglesias-Groth, S. 2007, *ApJ*, 661, L167
- [] Iglesias-Groth, S., & Esposito, M. 2013, *ApJ*, 776, L2
- [] Kharchenko, N. V., Scholz, R. D., Piskunov, A. E. et al. 2007, *Astron. Nachr.*, 328, 889
- [] Kroto, H. W., Heath, J. R., O'Brien, S. C. et al. 1985, *Nature*, 318, 162
- [] Kroto, H. W. & Jura, M. 1992, *A&A*, 263, 275
- [] Leger, A., & D'Hendecourt, L. 1985, *A&A*, 146, 81
- [] Luna, R., Cox, N. L. J., Satorre, M. A. et al. 2008, *A&A*, 480, 133
- [] McNabb, I. A., Fang, X., Liu, X. W. et al. 2013, *MNRAS*, 428, 3443
- [] Meixner, M., Skinner, C. J., Keto, E. et al. 1996, *A&A*, 313, 234
- [] Merrill, P. W., & Wilson, O. C. 1936, *AAS*, 8, 249
- [] Morisset, C., Szczerba, R., García-Hernández, D. A., García-Lario, P. 2012, in *Proc. IAU Symp. 283, Planetary Nebulae: An Eye to the Future*. Cambridge Univ. Press, Cambridge, eds. Manchado A., Stanghellini L., Schonberner D. p. 452
- [] Otsuka, M., Kemper, F., Cami, J. et al. 2014, *MNRAS*, 437, 2577
- [] Petrie, R. M., & Pearce, J. A. 1961, *Publications of the Dominion Astrophysical Observatory Victoria*, 12, 1
- [] Porceddu, I., Benvenuti, P., & Krelowski, J. 1991, *A&A*, 248, 188
- [] Pottasch, S. R., Bernard-Salas, J., Beintema, D. A. et al. 2004, *A&A*, 423, 593
- [] Pourbaix, D., Tokovinin, A. A., Batten, A. H. et al. 2004, *A&A*, 424, 727
- [] Rao, N. K., & Lambert, D. L. 1993, *MNRAS*, 263, L27
- [] Salama, F., Galazutdinov, G. A., Krelowski, J. et al. 1999, *ApJ*, 526, 265
- [] Sassara, A., Zerza, G., Chergui, M. & Leach, S. et al. 2001, *ApJ*, 135, 263
- [] Scarrott, S. M., Watkin, S., Miles, J. R. et al. 1992, *MNRAS*, 255, 11
- [] Seab, C. 1995, *The Diffuse Interstellar Bands*, Astrophysics and Space Science Library, 202, 129
- [] Sellgren, K., Werner, M. W., Ingalls, J. G. et al. 2010, *ApJ*, 722, L54
- [] Sharpee, B., Williams, R., Baldwin, J. A. et al. 2003, *ApJS*, 149, 157
- [] Snow, T. P., Zukowski, D., & Massey, P. 2002, *ApJ*, 578, 877
- [] Snow, T. P., & McCall, B. J. 2006, *ARA&A*, 44, 367
- [] Snow, T. P., & Destree, J. D. 2011, *EAS*, 46, 341
- [] Tielens, A. G. G. M. 2005, *The Physics and Chemistry of the Interstellar Medium* (Cambridge University Press)
- [] Tielens, A. G. G. M. 2008, *ARA&A*, 46, 289
- [] Van der Zwet, G. P., & Allamandola, L. J. 1985, *A&A*, 146, 76
- [] van Loon, J. Th., Bailey, M., Tatton, B. L. et al. 2013, *A&A*, 550, 108
- [] Wang, W., & Liu, X.-W. 2007, *MNRAS*, 381, 669
- [] Watson, J. K. G. 1994, *ApJ*, 437, 678
- [] Wegner, W. 2003, *AN*, 324, 219
- [] Weisman, J. L., Lee, T. J., Salama, F. et al. 2003, *ApJ*, 587, 256
- [] Williams, R., Jenkins, E. B., Baldwin, J. A. et al. 2008, *ApJ*, 677, 1100
- [] Wilson, O. C. 1953, *ApJ*, 117, 264
- [] Zhang, Y., & Kwok, S. 2011, *ApJ*, 730, 126

Appendix A: Tables A1, A2, A3, A4, A5, and A6.

Table A.1. Diffuse interstellar bands in Tc 1 and HR 6334.^a

Tc 1					HR 6334						
λ_c (Å)	Components (Å)	FWHM (Å)	EQW (mÅ)	S/N	EQW/ E_{B-V} (Å/mag)	λ_c (Å)	Components (Å)	FWHM (Å)	EQW (mÅ)	S/N	EQW/ E_{B-V} (Å/mag)
4427.51 ^{b,c}	...	19.35	860.0	403	3.74	4429.71	...	23.42	470.2	391	1.12
5776.22	...	1.14	7.2	402	0.03	5776.11	...	1.21	5.3	535	0.01
5780.65 ^c	...	2.02	112.1	420	0.49	5780.59	...	2.17	119.0	586	0.28
5797.21	...	0.82	25.7	536	0.11	5797.19	...	1.15	45.7	590	0.11
5849.74	...	0.89	2.2	437	0.01	5849.74	...	0.76	12.7	536	0.03
6196	6196.06 ^d	1.11	10.7	525	0.05	6196	6196.05 ^d	0.96	16.0	692	0.04
	6195.88	0.48	6.0		0.03		6195.89	0.40	10.4		0.02
	6196.54	0.39	2.6		0.01		6196.56	0.36	4.3		0.01
6203.33	...	2.03	36.7	560	0.16	6203.17	...	1.28	29.1	758	0.07
6250.36	...	1.74	8.7	610	0.04	6250.62	...	2.45	14.7	727	0.03
6270.08	...	1.66	15.0	618	0.06	6270	6269.98	1.47	25.8	494	0.06
6284.18	...	4.41	630	380	1.66	6284.15	...	4.55	309.8	693	0.74
6376	6376.22 ^d	1.38	2.6	559	0.01	6376	6376.40 ^d	1.36	12.7	612	0.03
	6376.05	0.57	1.7		0.01		6375.92	0.41	3.6		0.01
	6376.76	0.48	1.6		0.01		6376.65	0.76	6.4		0.01
6379	6379.41 ^d	1.13	8.7	625	0.04	6379	6379.47 ^d	1.26	56.4	812	0.13
	6379.14	0.56	4.9		0.02		6379.14	0.46	21.0		0.05
	6379.82	0.93	4.7		0.02		6379.78	1.08	35.4		0.08
6597.18	...	0.48	4.1	529	0.02	6597.14	...	0.45	5.0	338	0.01
6613.77	...	1.47	32.5	432	0.14	6613.74	...	1.40	91.8	464	0.22
6661	6661.09 ^d	1.12	3.5	341	0.01	6661	6660.81 ^d	1.09	22.8	337	0.05
	6660.64	0.64	2.5		0.01		6660.61	0.54	14.4		0.03
	6661.40	0.24	1.9		0.01		6661.35	0.30	5.4		0.01
6792.22	...	1.16	12.6	360	0.05	6792.07	...	1.10	15.2	329	0.04
7828.75	...	1.49	8.8	382	0.04	7828.45	...	1.07	6.1	572	0.01
7832.50	...	1.76	10.3	475	0.04	7832.63	...	2.11	14.5	636	0.03
8038.14	...	0.96	5.4	396	0.02	8038.01	...	0.81	7.0	460	0.02
8621.12	...	4.52	63.4	348	0.28	8621.15	...	4.50	51.7	626	0.12

Notes.

^(a) The $3\text{-}\sigma$ errors in the EQWs scale as $\sim 3 \times \text{FWHM}/(\text{S/N})$, while we estimate that the FWHMs in Tc 1 are precise to the 0.03 \AA level (less for M 1-20 and IC 418).

^(b) The parameters of this DIB are estimated by adopting a Lorentzian profile (see, e.g., Snow et al. 2002).

^(c) Circumstellar absorption features (or diffuse circumstellar bands) may be possibly detected at these wavelengths (see Section 4).

^(d) Undeblended DIB.

Table A.2. Diffuse interstellar bands in M 1-20 and HR 6716.^a

M 1-20					HR 6716					
λ_c (Å)	FWHM (Å)	EQW (mÅ)	S/N	EQW/ E_{B-V} (Å/mag)	λ_c (Å)	FWHM (Å)	EQW (mÅ)	S/N	EQW/ E_{B-V} (Å/mag)	
4426.56 ^b	19.94 ^c	2579.0 ^c	20 ^d	3.22	4429.27	22.25	595.8	233	2.71	
5780.44	1.93	361.1	36	0.45	5780.41	2.01	164.5	792	0.75	
5796.97	0.78	153.4	39	0.19	5796.95	0.74	37.2	661	0.17	
5849.69	0.95	70.7	52	0.09	5849.69	0.84	9.3	639	0.04	
6195.83	0.43	44.3	71	0.05	6195.82	0.41	13.2	612	0.06	
6203.00	1.39	97.7	77	0.12	6203.02	1.25	28.9	688	0.13	
6269.89	1.51	89.2	67	0.11	6269.70	1.02	12.4	684	0.06	
6283.60	4.06	573.0	73	0.72	6283.51	4.29	474.4	641	2.16	
6375.94	0.51	26.3	75	0.03	6375.89	0.65	6.3	656	0.03	
6379.14	0.59	80.6	100	0.10	6379.12	0.63	22.5	687	0.10	
6613.48	1.01	177.0	79	0.22	6613.41	0.86	37.5	581	0.17	
6660.52	0.59	27.5	74	0.03	6660.55	0.41	5.0	531	0.02	

Notes.

^(a) The $3\text{-}\sigma$ errors in the EQWs scale as $\sim 3 \times \text{FWHM}/(\text{S/N})$, while the FWHMs are less precise than 0.03 \AA .

^(b) The parameters of this DIB are estimated by adopting a Lorentzian profile (see, e.g., Snow et al. 2002). The central wavelength in M 1-20 is very uncertain.

^(c) Best estimates found by clipping out the narrow emission lines and smoothing the spectrum with boxcar 15. The error in the quoted EQW is estimated to be $\sim 786 \text{ mÅ}$.

^(d) S/N in the original spectrum.

Table A.3. Diffuse interstellar bands in IC 418 and HR 1890.^a

IC 418					HR 1890					Hobbs et al. (2008)		Luna et al.(2008)
λ_c (Å)	FWHM (Å)	EQW (mÅ)	S/N	EQW/E _{B-V} (Å/mag)	λ_c (Å)	FWHM (Å)	EQW (mÅ)	S/N	EQW/E _{B-V} (Å/mag)	EQW/E _{B-V} (Å/mag)	EQW/E _{B-V} (Å/mag)	
4426.20 ^b	21.45	1001.0	116	4.35	1.10	...	
5780.94	2.02	99.8	195	0.43	5780.97	1.68	25.5	344	0.32	0.23	0.46	
5797.51	0.85	34.8	184	0.15	5797.46	1.07	8.4	336	0.10	0.18	0.17	
5850.55	1.15	30.9	175	0.13	5850.44	1.03	7.1	351	0.09	0.09	0.061	
6196.47	0.31	10.0	166	0.04	6196.27	0.29	2.9	343	0.04	0.03	0.053	
6203.37	0.80	15.3	171	0.07	0.05	...	
6270.24	1.08	15.7	183	0.07	0.07	...	
6284.30	4.88	218.8	183	0.95	0.41	0.90	
6376.41	0.35	2.9	137	0.01	0.04	...	
6379.94	0.43	5.2	132	0.02	0.08	0.088	
6614.11	1.04	30.8	146	0.13	6614.20	0.91	6.6	364	0.08	0.15	0.21	

Notes.
^(a) The 3- σ errors in the EQWs scale as $\sim 3 \times \text{FWHM}/(\text{S/N})$, while the FWHMs are less precise than 0.03 Å.

^(b) The parameters of this DIB are estimated by adopting a Lorentzian profile (see, e.g., Snow et al. 2002). The quoted central wavelength in IC 418 is quite uncertain.

Table A.4. Radial velocities (in kms^{-1}) for the atomic and molecular lines as well as DIB features with two interstellar components in Tc 1 and HR 6334.^a

Feature	Tc 1		HR 6334	
	CS	IS	IS	IS
Na I	-116.10	-83.00	-4.67	26.36
Ca I			-7.16	22.98
CH ⁺			-6.87	25.50
CH				-2.83
CN (R1)				-5.86
CN (R0)				27.96
CN (P1)				-5.34
DIB 6196Å				(42)
DIB 6376Å				-4.57
DIB 6379Å				29.25
				-4.18
				31.02
				-8.03
				25.11
				-5.42
				27.68
				-3.86
				30.00
				-7.05
				33.34
				-6.58
				23.97
				-5.78
				29.18

Notes.
^(a) Typical uncertainty of $\sim \pm 1 \text{ kms}^{-1}$.

Table A.5. Radial velocities (in kms^{-1}) for the atomic lines as well as DIB features in M 1-20 and HR 6716.^a

Feature	M 1-20		HR 6716	
	CS	IS	IS	IS
Na I	60.95?	-6.54	-26.43	-6.12
DIB 5797Å		-5.19		-5.33
DIB 6196Å		-7.85		-7.88
DIB 6379Å		-8.63		-9.04

Notes.
^(a) Typical uncertainty of $\sim \pm 1 \text{ kms}^{-1}$.

Table A.6. Radial velocities (in kms^{-1}) for the atomic and molecular lines, as well as DIB features in IC 418 and HR 1890.^a

Feature	IC 418		HR 1890	
	CS	IS	IS	IS
Na I	58.36	22.22	5.42	23.75
CH		22.67		
DIB 5780Å		25.34		23.33
DIB 5797Å		22.16		22.15
DIB 5850Å		25.60		30.97

Notes.
^(a) Typical uncertainty of $\sim \pm 1 \text{ kms}^{-1}$.